Development 140, 237-246 (2013) doi:10.1242/dev.084111

Visualization of cell cycle in mouse embryos with Fucci2 reporter directed by *Rosa26* promoter

Takaya Abe[1], Asako Sakaue-Sawano[2,3], Hiroshi Kiyonari[1], Go Shioi[1], Ken-ichi Inoue[1], Toshitaka Horiuchi[4], Kazuki Nakao[1,5], Atsushi Miyawaki[2,3], Shinichi Aizawa[1,*] and Toshihiko Fujimori[1,6]

SUMMARY

Fucci technology makes possible the distinction between live cells in the G_1 and S/G_2/M phases by dual-color imaging. This technology relies upon ubiquitylation-mediated proteolysis, and transgenic mice expressing Fucci provide a powerful model system with which to study the coordination of the cell cycle and development. The mice were initially generated using the CAG promoter; lines expressing the G_1 and S/G_2/M phase probes that emitted orange (mKO2) and green (mAG) fluorescence, respectively, were separately constructed. Owing to cell type-biased strength of the CAG promoter as well as the positional effects of random transgenesis, however, we noticed some variability in Fucci expression levels. To control more reliably the expression of cell cycle probes, we used different genetic approaches to create two types of reporter mouse lines with Fucci2 and *Rosa26* transcriptional machinery. Fucci2 is a recently developed Fucci derivative, which emits red (mCherry) and green (mVenus) fluorescence and provides better color contrast than Fucci. A new transgenic line, *R26p-Fucci2*, utilizes the *Rosa26* promoter and harbors the G_1 and S/G_2/M phase probes in a single transgene to preserve their co-inheritance. In the other *R26R-Fucci2* approach, the two probes are incorporated into *Rosa26* locus conditionally. The Cre-mediated *loxP* recombination technique thus allows researchers to design cell-type-specific Fucci2 expression. By performing time-lapse imaging experiments using *R26p-Fucci2* and *R26-Fucci2* in which *R26R-Fucci2* had undergone germline *loxP* recombination, we demonstrated the great promise of these mouse reporters for studying cell cycle behavior *in vivo*.

KEY WORDS: Rosa26 reporter mouse, Cell cycle indicator, Live imaging

INTRODUCTION

Visualization of the progress of the cell cycle in cells of live embryos provides valuable information for understanding developmental processes such as pattern formation, morphogenesis, cell differentiation, growth, cell migration and cell death. Sakaue-Sawano et al. (Sakaue-Sawano et al., 2008) developed a fluorescent ubiquitylation-based probe, called the fluorescent ubiquitylation-based cell cycle indicator (Fucci), to visualize the cell cycle in live cells. The Fucci probe was generated by fusing monomeric Kusabira Orange 2 (mKO2) (Karasawa et al., 2004) and monomeric Azami Green (mAG) (Karasawa et al., 2003) to the ubiquitylation domains of human Cdt1 [hCdt1(30/120)] and Geminin [hGem(1/110)], respectively. These two chimeric proteins, mKO2-hCdt1(30/120) and mAG-hGem(1/110), accumulate reciprocally in the nuclei during the cell cycle, labeling the nuclei of G_1 phase cells in orange and those of S, G_2 and M phase cells in green. Thus, they function as G_1 and S/G_2/M probes, respectively. Subsequently, to improve the imaging quality, Fucci2 was developed with a green monomeric variant of *Aequoea* green fluorescent protein (mVenus) (Nagai et al., 2002) and a red monomeric fluorescent protein (mCherry) (Shaner et al., 2004); mCherry and mVenus were conjugated to hCdt1(30/120) and hGem(1/110) to generate mCherry-hCdt1(30/120) and mVenus-hGem(1/110), respectively (Sakaue-Sawano et al., 2011). The mCherry red fluorescence is separated from the green fluorescence more clearly than the mKO2 orange fluorescence, and mVenus exhibits much brighter green fluorescence than mAG.

To visualize the cell cycle in living cells of embryos or animals, two mouse lines, *CAG-mKO2-hCdt1*(*30/120*) and *CAG-mAG-hGem*(*1/110*), were initially generated by random transgenesis (Sakaue-Sawano et al., 2008). The *CAG-Fucci* mouse line that co-harbors *CAG-mKO2-hCdt1*(*30/120*) and *CAG-mAG-hGem*(*1/110*) was obtained by crossing the two transgenic lines, and successfully used to monitor the cell cycle in the head region of embryonic day (E) 13 embryos; regional differences in cell proliferation activities were demonstrated in the neural tissue. However, it is laborious to maintain the two probes together. In addition, *CAG* is a conventional ubiquitous promoter of a viral origin for transgenic studies (Niwa et al., 1991), and it is inactive or only weakly active in several tissues (Rhee et al., 2006; Griswold et al., 2011). The random nature of integration sites exacerbates this problem of the *CAG* promoter. Indeed, signals are too weak to analyze the cell cycle in cleavage stage embryos and several tissues, such as extra-embryonic tissues in early post-implantation embryos, of the *CAG-Fucci* line.

To develop mouse cell cycle reporter lines for wider use, here we took two different approaches using Fucci2 probes [*mCherry-hCdt1*(*30/120*) and m*Venus-hGem*(*1/110*)] and *Rosa26* locus; the locus has been known to be the most ubiquitous endogenous locus, and its disruption to cause no apparent defects (Friedrich and Soriano, 1991; Zambrowicz et al., 1997; Soriano, 1999; Srinivas et al., 2001). One is a transgenic *R26p-Fucci2* approach in which *Rosa26* promoter (*R26p*) bidirectionally directs *mCherry-*

[1]Laboratory for Animal Resources and Genetic Engineering, RIKEN Center for Developmental Biology (CDB), Kobe 650-0047, Japan. [2]Life Function and Dynamics, ERATO, JST, 2-1 Hirosawa, Wako-city, Saitama 351-0198, Japan. [3]Laboratory for Cell Function and Dynamics, Advanced Technology Development Group, Brain Science Institute, RIKEN, 2-1 Hirosawa, Wako-city, Saitama 351-0198, Japan. [4]Faculty of Life and Environmental Sciences, Department of Life Sciences Prefectural University of Hiroshima, Shobara 727-0023, Japan. [5]Laboratory of Animal Resources, Center for Disease Biology and Integrative Medicine Faculty of Medicine (CDBIM), University of Tokyo, Tokyo 113-0033, Japan. [6]Division of Embryology, National Institute for Basic Biology (NIBB), Okazaki 444-8787, Japan.

*Author for correspondence (saizawa@cdb.riken.jp)

Accepted 24 September 2012

hCdt1(*30/120*) and *mVenus-hGem*(*1/110*) in a single transgene. In the other *R26R-Fucci2* approach, *mCherry-hCdt1*(*30/120*) and *mVenus-hGem*(*1/110*) were inserted into *Rosa26* locus conditionally, placing a *loxP*-flanked stop sequence in front of each of them [*R26R-mCherry-hCdt1*(*30/120*) or *R26R-mVenus-hGem*(*1/110*)] to silence the probes (Srinivas et al., 2001). The *loxP* recombination in the *R26R* lines by crossing with *EIIa-Cre* (Lakso et al., 1996) mice yielded *R26* lines in which the stop sequence is lost and the probes are ubiquitously expressed. The *R26-mCherry-hCdt1*(*30/120*) and *R26-mVenus-hGem*(*1/110*) mouse lines are maintained in a homozygous state; their cross yields the *R26-Fucci2* embryos, of which one *Rosa26* allele harbors *mCherry-hCdt1*(*30/120*) and the other allele *mVenus-hGem*(*1/110*) (*Rosa26*$^{mCherry\text{-}hCdt1(30/120)/mVenus\text{-}hGem(1/110)}$). The analysis in early embryos demonstrated that the *R26-Fucci2* is indeed useful in monitoring cell cycle behaviors *in vivo*. The parental, conditional *R26R-Fucci2* is appropriate for the cell cycle analysis in a specific population of the cells.

MATERIALS AND METHODS

Generation of *R26p-Fucci2* mouse line

mCherry-hCdt1(*30/120*) and *mVenus-hGem*(*1/110*) cDNAs were obtained from *pcDNA3-mCherry-hCdt1*(*30/120*) and *pcDNA3-mVenus-hGem*(*1/110*) (Sakaue-Sawano et al., 2011) and recloned into *pENTR L1-L4* and *pENTR L3-L2* vectors containing the bovine growth hormone polyadenylation sequence, respectively. The *2xcHS4* fragment was obtained from *UBC-HS-RG* (Stewart et al., 2009), and recloned into the *pENTR R4-R3*. The Reading Frame Cassette A of the Gateway Conversion System (Invitrogen) was flanked by *2xcHS4* and *Rosa26* promoter (*R26p*) (Kisseberth et al., 1999) fragments to generate *pBidirectional-R26p-DEST*. The three DNA fragments in the *pENTR* vector were recloned into *pBidirectional-R26p-DEST* using LR clonase of the Gateway System to generate the *R26p-Fucci2* transgene (supplementary material Fig. S5). The transgene was released from its plasmid backbone by *Kpn*I and *Sac*I digestion and isolated by electrophoresis and gel purification using the Gel and PCR clean-up system (Promega). The purified transgene DNA was eluted with TE (10 mM Tris, 1 mM EDTA, pH 8.0) buffer, diluted with PBS (–) buffer to a final concentration of 5 ng/μl and injected into pronuclei of BDF1 (C57BL/6N × DBA/2N) zygotes as described (http://www.cdb.riken.jp/arg/Methods.html). Four transgenic lines were screened for their fluorescent intensities with E7.5 hemizygous F1 or F2 embryos, and a transgenic line termed *R26p-Fucci2* (accession no. CDB0203T; http://www.cdb.riken.jp/arg/reporter_mice.html) was selected for the present analysis. The transgenic line was successively backcrossed with C57BL/6N; mice or embryos were genotyped by PCR with the primers 5′-ATG GTG AGC AAG GGC GAG GAG-3′ and 5′-CTT GTA CAG CTC GTC CAT GCC G-3′ for *mVenus*, and the primers 5′-GCT TCA AGG TGC ACA TGG AG-3′ and 5′-CAT GAA CTG AGG GGA CAG GA-3′ for *mCherry*, yielding 717 bp and 161 bp products, respectively.

Establishment of *Rosa26* knock-in mice

Targeting vectors were constructed, homologous recombinant embryonic stem (ES) cells were isolated and chimeric mice were generated as described (Abe et al., 2011). In brief, the vectors were constructed by the Gateway Recombination System (Invitrogen) (Abe et al., 2011). *mCherry-hCdt1*(*30/120*) and *mVenus-hGem*(*1/110*) cDNAs obtained from *pcDNA3-mCherry-hCdt1*(*30/120*) and *pcDNA3-mVenus-hGem*(*1/110*) were cloned into the *pENTR2B* vector (Invitrogen). Each cDNA in the *pENTR2B* vector was recloned into *pROSA26-STOP-DEST* using LR clonase of the Gateway System, respectively, generating each targeting vector. They were introduced into TT2 ES cells (Yagi et al., 1993b) by electroporation, and 48 G418-resistant colonies were screened for homologous recombinants on each vector by PCR (Fig. 3A), identifying 15 and 18 colonies as homologous recombinant for *R26R-mCherry-hCdt1*(*30/120*) and *R26R-mVenus-hGem*(*1/110*), respectively. The size of the products and primers used were: 3.6 kb with forward primer P1, 5′-GAA AGA ACC AGC TGG GGC TCG ATC C-3′, and reverse primer P2, 5′-TTG ACT CCT AGA CTT GTG ACC CAG C-3′. Homologous recombination was confirmed by Southern hybridization; digesting with *Afl*II, the 485 bp probe (indicated in Fig. 3A) detected a 13.3 kb band for wild-type allele and a 17.7 kb band for the targeted allele on both *R26R-mCherry-hCdt1*(*30/120*) and *R26R-mVenus-hGem*(*1/110*); the probe was prepared by PCR with primers 5′-ACA GTG TAC CAA GAG TGG-3′ and 5′-GCT GGT TTT TCT AGC TCC-3′. The homologous recombinant TT2 ES cells were injected into eight-cell stage ICR embryos to generate germline chimera, which were mated with C57BL/6N females to yield *R26R-mCherry-Cdt1*(*30/120*) (accession no. CDB0229K) and *R26R-mVenus-hGem*(*1/110*) (accession no. CDB0230K) lines (http://www.cdb.riken.jp/arg/reporter_mice.html). Their *R26* mouse lines, *R26-mCherry-hCdt1*(*30/120*) (accession no. CDB0264K) and *R26-mVenus-hGem*(*1/110*) (accession no. CDB0265K) (http://www.cdb.riken.jp/arg/reporter_mice.html), that ubiquitously express mCherry-hCdt1(30/120) and mVenus-hGem(1/110) proteins, respectively, were obtained by crossing each *R26R* mouse line with an *EIIa-Cre* C5379Lmgd/J transgenic mouse harboring Cre under the *EIIa* promoter (Lakso et al., 1996). Offspring and embryos were routinely genotyped by PCR: wild-type allele, 217 bp products with forward P3 (5′-TCC CTC GTG ATC TGC AAC TCC AGT C-3′) and reverse P4 (5′-AAC CCC AGA TGA CTA CCT ATC CTC C-3′); R26R allele, 385 bp products with forward P3 and reverse P5 (5′-TGT GGA ATG TGT GCG AGG CCA GAG G-3′); R26 allele, 270 bp products with forward P3 and reverse P6 (5′-GCT GCA GGT CGA GGG ACC-3′). Primers to detect *mCherry-hCdt1*(*30/120*) and *mVenus-hGem*(*1/110*) transgenes are as described above.

Marker mouse lines

R26-H2B-EGFP (accession no. CDB0238K), *R26-H2B-mCherry* (accession no. CDB0239K), FucciG_1-#596 [*CAG-mKO2-hCdt1*(*30/120*)] and FucciS/G_2/M-#504 [*CAG-mAG-hGem*(*1/110*)] mouse lines were previously generated (Abe et al., 2011; http://www.cdb.riken.jp/arg/reporter_mice.html) (Niwa et al., 1991; Sakaue-Sawano et al., 2008).

Cell cycle analysis by EdU labeling

Fertilized eggs were obtained by *in vitro* fertilization between C57BL/6N eggs and *R26p-Fucci2* sperms, cultured to the two-cell stage and stocked in frozen. For 5-ethynyl-2′-deoxyuridine (EdU) labeling, the frozen embryos were thawed and cultured in KSOM medium; 20 μM EdU was added to the medium at the 16-cell stage, and the embryos were cultured for 30 minutes before the fixation. The cells incorporating EdU were detected using Click-iT EdU Alexa Fluor 647 Imaging Kit (Invitrogen) according to the manufacturer's protocol. To detect mCherry-hCdt1(30/120) and mVenus-hGem(1/110) by immunostaining, the EdU-labeled embryos were incubated for 1 hour at 4°C in PBS (–) with 0.1% Triton X-100 and 5% donkey serum and then for overnight with anti-GFP (rat monoclonal, Nacalai Tesque) and anti-DsRed (rabbit polyclonal, Clontech) antibodies. After washing three times with PBS (–) containing 0.1% Triton X-100, the embryos were further incubated at 4°C for overnight with anti-rat antibodies coupled with Alexa Fluor 488 (donkey polyclonal, Molecular Probes), anti-rabbit antibodies coupled with Cy3 (donkey polyclonal, Jackson ImmunoResearch) and Hoechst 33342 (5 μg/ml). The embryos were then washed three times with PBS (–) containing 0.1% Triton X-100.

Imaging of embryos

For time-lapse imaging, fertilized eggs were collected in KSOM medium and cultured in an atmosphere of 5% CO_2 at 37°C. The images were obtained with the Olympus incubation imaging system LCV100 equipped with CSU10 (YOKOGAWA) and an iXon+EMCCD camera (Andor); filters used were a band-pass filter (Olympus, 495-540 nm) for mVenus and a long-pass filter (575 nm) for mCherry in supplementary material Movies 1 and 2, and a triple band filter (YOKOGAWA, transmission: 495-555 nm, 575-635 nm, and 665-775 nm) in supplementary material Movies 3-7. The images at every 10-minute interval with nine *z*-sections were analyzed by MetaMorph software (Universal Imaging Corporation); the *z*-section interval was 5 μm. The nuclei enclosed as region of interest (ROI) cover about 80% of the region of nuclear signals to determine fluorescent intensities.

To determine fluorescent images of embryos from E5.5 to E9.5, the embryos were dissected in DMEM medium without phenol red and imaged by an A1-Ti confocal microscope (Nikon) (filters used were a band-pass filter 425/50 for Hoechst, a band-pass filter 525/50 for mVenus, a band-pass filter 595/50 for mCherry and a band-pass filter 700/75 for Alexa Fluor 647), or by Macro Confocal Laser Microscope System AZ-C1 (Nikon) (filters used were a band-pass filter 515/30 for mVenus and a band-pass filter 605/75 for mCherry). The 405, 488, 561 and 640 nm lasers were used to obtain Hoechst, mVenus, mCherry and Alexa Fluor 647 fluorescent images, respectively.

E13.5 embryos obtained by crossing C57BL/6N female with *R26p-Fucci2* male were fixed with 4% paraformaldehyde at 4°C for overnight. For the whole embryo imaging, fixed embryos were incubated at 4°C for 2 weeks in SCALEVIEW-A2 (OLYMPUS) (Hama et al., 2011), the buffer was changed several times, and imaged by a Macro Confocal Laser Microscope System AZ-C1 (Nikon). To make frozen sections, fixed embryos were equilibrated in PBS (-) with 20% sucrose, embedded in optimal cutting temperature compound (OCT; TissueTek) and frozen. The frozen blocks were sectioned by a cryostat into 12 μm thicknesses. mVenus green fluorescence was lost by the fixation, and the two Fucci2 signals in the frozen sections were observed by immunostaining as described above (supplementary material Fig. S3C-G). They were imaged by an A1-Ti confocal microscope (Nikon).

RESULTS

Generation of bidirectional *R26p-Fucci2* mice

CAG-Fucci transgenic mice have been successfully used to monitor the cell cycle *in vivo* (Sakaue-Sawano et al., 2008). However, the intensities of the probes were not high enough in several tissues of mouse embryos such as blastomeres at early cleavage stage and extra-embryonic tissues (supplementary material Fig. S1). We then sought to develop a new reporter mouse line for cell cycle analysis with Fucci2, and chose a promoter of *Rosa26* locus (*R26p*) to direct the probe expression (Kisseberth et al., 1999); the promoter is a ubiquitous promoter of mouse genome origin. Furthermore, the *CAG-Fucci* line harbors two probes in different chromosomes; it is laborious to maintain the two probes in the *CAG-Fucci* line and to analyze the cell cycle with this line in a mutant background. To overcome this problem, the two probe genes of Fucci2, *mCherry-hCdt1*(*30/120*) and *mVenus-hGem*(*1/110*), were put into a single transgene (Fig. 1A,B); in the transgene, *mCherry-hCdt1*(*30/120*) and *mVenus-hGem*(*1/110*), each driven by *R26p,* were conjugated bidirectionally, being separated by two copies of chicken hypersensitive site 4 (*cHS4*) transcriptional insulators. The insulators were also placed at both ends of the transgene to minimize positional effects of the transgene integration site (Potts et al., 2000; Stewart et al., 2009).

Examination of their fluorescent intensities in E7.5 F1 hemizygous embryos resulted in selection of a transgenic line called *R26p-Fucci2* for the further characterization. The hemizygous embryos in this line exhibited distinct fluorescent activities not only in embryonic tissues but also in blastomeres at early cleavage stages and in extra-embryonic tissues as described below. The *R26p-Fucci2* mouse line is maintained in the hemizygous state; no homozygous mice were identified among more than 100 pups obtained by the hemizygous crosses.

Cell cycle behaviors of Fucci2 probes in *R26p-Fucci2* embryos at 16-cell stage

Previous studies in cell culture have demonstrated that mCherry-hCdt1(30/120) signal occurs in nuclei at early G_1 phase, starts to decrease with the transition from G_1 to S phase, and disappears at the S phase; by contrast, the mVenus-hGem(1/110) signal occurs in nuclei at early S phase, increases toward M phase, and disappears rapidly in late M phase (Sakaue-Sawano et al., 2011). To confirm that this is also true *in vivo*, we have conducted cell cycle analysis of *R26p-Fucci2* embryos at the 16-cell stage by EdU labeling. Two examples of confocal images of these embryos are given in Fig. 1C and 1D. There is a gap phase at the time of cell division in which both green and red fluorescences are absent. The green fluorescence in nuclei was lost and distributed over the cytoplasm with the breakdown of nuclear envelope at prometaphase of M phase. APC^{Cdh1} complex that degrades Geminin by ubiquitylation is activated at anaphase (Vodermaier, 2004); the green fluorescence in cytoplasm disappeared in late M phase (Sakaue-Sawano et al., 2008). The red fluorescence occurs in the daughter cells soon after the division or in early G_1 phase. The activation of SCF^{Skp2} complex that degrades Cdt1 by ubiquitylation occurs at the onset of S phase (Vodermaier, 2004); the S phase starts at around the time point when the red fluorescence peaks. During red-to-green conversion, there was a phase when cells emitted both red and green fluorescence (Fig. 1C,D); the cells yield yellow nuclei in merged (mCherry/mVenus) views (Fig. 1D; supplementary material Movies 3, 4, 7). All of these cells showed EdU incorporation (purple nuclei), and were in early S phase (G_1/S transition phase) (Sakaue-Sawano et al., 2008). Subsequently, the cells lost red fluorescence with moderate green fluorescence. These cells also incorporated EdU, and were in S phase. Then the cells became intensively green fluorescent; these cells did not incorporate EdU and were in G_2 phase. Consequently, the cells are in G_1 phase when nuclei have only red fluorescence and in S, G_2 and M phases when nuclei have only green fluorescence. Both fluorescent signals are lost at late M phase but present in early S phase (Fig. 1G). The results are consistent with the previous study in cultured cells (Sakaue-Sawano et al., 2011).

Time-lapse observation of *R26p-Fucci2* preimplantation embryos

Time-lapse imaging of the *R26p-Fucci2* 16-cell stage embryos is shown in supplementary material Movie 4, and Fig. 1E,F shows their snapshot images. Two examples of the quantification of the signals over one cell cycle are shown in Fig. 1G. The variation in signal intensity among cells of the embryo appeared minimal, if any. The signal intensities are adequate to monitor the cell cycle in each cell of the embryo, and no less sufficient than that of the *CAG-Fucci* mouse line (Sakaue-Sawano et al., 2008).

Fucci2 signals at earlier developmental stages are shown in supplementary material Fig. S2 and Movies 1, 3, 4 with the embryos in which the *R26p-Fucci2* transgene was transmitted maternally. Mature oocytes expressed mCherry-hCdt1(30/120) abundantly over ooplasm, whereas they did not mVenus-hGem(1/110) at all (supplementary material Fig. S3H-I′). After fertilization the mCherry-hCdt1(30/120) signal was strongly observed in both female and male pronuclei (supplementary material Movies 1, 2). The signal dispersed over cytoplasm, probably with the breakdown of pronuclear envelope at syngamy. A strong signal came back in the nuclei of the two-cell stage embryo after cell division or G_1 phase (supplementary material Movie 2), and the signal in cytoplasm was greatly reduced; the peak intensity of mCherry-hCdt1(30/120) signal in nuclei at the two-cell stage was about 50-fold that of the 16-cell stage. The mCherry signal began to decrease at about 1.5 hours after the cell division; consistent with the length of G_1 described in previous reports (Luthardt and Donahue, 1975; Molls et al., 1983; Smith and Johnson, 1986). However, significant mCherry signals remained in

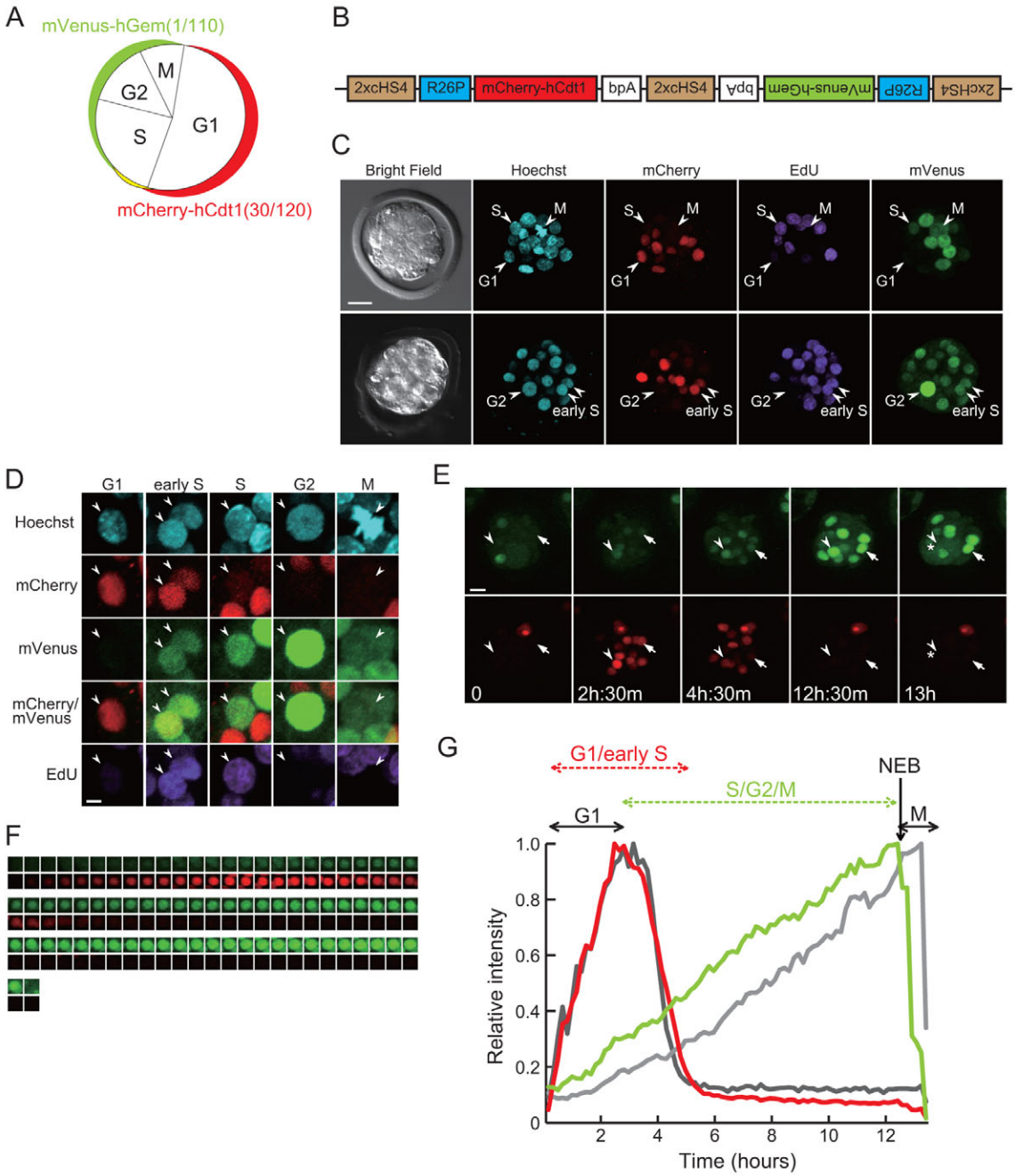

Fig. 1. Cell cycle observation at the 16-cell stage by *R26p-Fucci2* line. (**A**) Diagram of the expression of Fucci2 probes in nuclei. mCherry-hCdt1(30/120) probe labels G_1 and early S phase nuclei in red, and mVenus-hGem(1/110) probe S, G_2 and M phase nuclei in green. Yellow indicates co-existence of red and green signals. (**B**) *R26p-Fucci2* transgene construct. *mCherry-hCdt1(30/120)* and *mVenus-hGem(1/110)* each driven by *R26p* are conjugated bidirectionally, being separated by two copies of *cHS4* transcriptional insulator. The insulator is also placed at both ends of the transgene. *2xcHS4*, chicken hypersensitive site 4; *bpA*, bovine growth hormone polyadenylation sequence; *R26p*, *Rosa26* promoter. (**C**) Three-dimensional confocal projection images of *R26p-Fucci2* embryos labeled with EdU during the 16-cell stage. Two examples are shown among 28 hemizygous embryos analyzed; all gave the same pattern. Scale bar: 20 μm. (**D**) Higher magnification images of the nuclei and chromosomes indicated by arrowheads in C. Red and green signals represent mCherry-hCdt1(30/120) and mVenus-hGem(1/110) expression, respectively. In merged (mCherry/mVenus) views, yellow signals indicate the cells that express both mCherry-hCdt1(30/120) and mVenus-hGem(1/110). EdU-incorporated nuclei are represented in purple; Hoechst signals in cyan. Scale bar: 5 μm. (**E**) Snapshot images of a time-lapse observation during the 16-cell stage. White arrowheads and arrows indicate nuclei that are tracked. An asterisk indicates a cell division. Scale bar: 20 μm. (**F**) Higher magnification images of a nucleus indicated by arrowheads in E at 10-minute intervals. (**G**) Changes in signal intensities of Fucci2 probes during the 16-cell stage. mCherry-hCdt1(30/120) and mVenus-hGem(1/110) signals in the nucleus indicated by white arrowheads in E are shown by red and green lines, respectively, and the nucleus indicated by white arrows in black and gray lines, respectively. The peak intensities of mCherry and mVenus during the 16-cell stage are each set to 1.0, and each intensity at each time point is given as the relative value to them. mCherry signals accumulated in nuclei during G_1 phase and gradually decreased in early S phase. By contrast, the mVenus signals in nuclei increased toward prometaphase, and lost by dispersion over the cytoplasm with nuclear envelope breakdown (NEB); mVenus signals remained in the cytoplasm until late M phase.

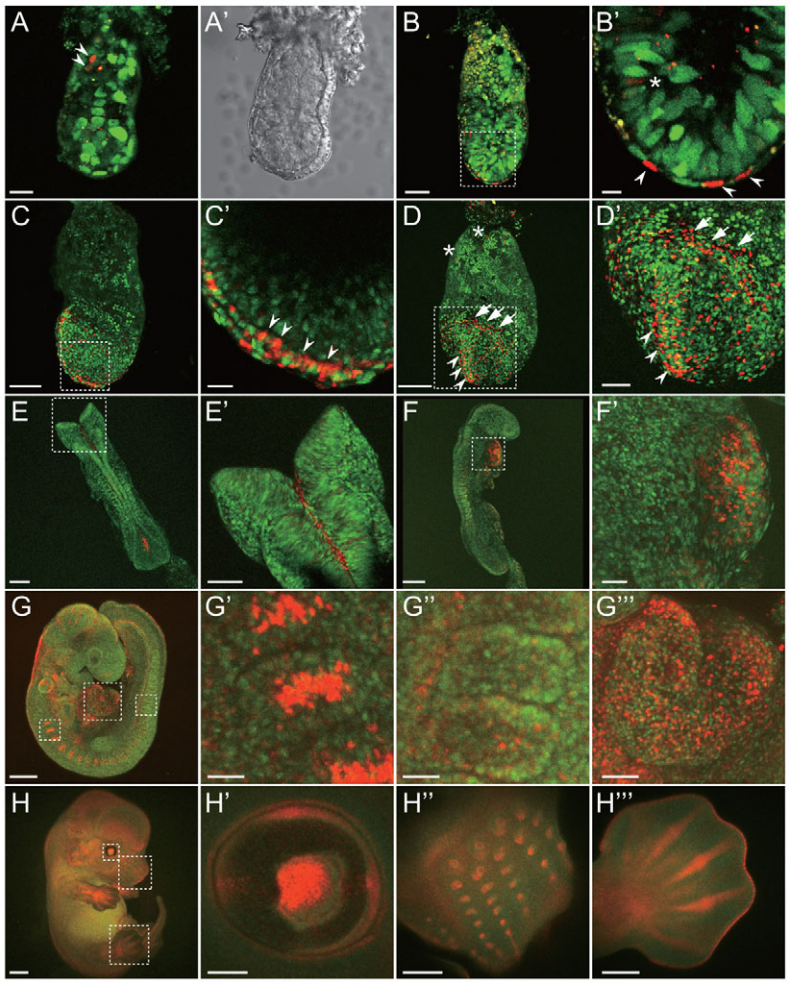

Fig. 2. Fucci2 signals in *R26p-Fucci2* embryos after implantation. (**A-H‴**) Projection of *z*-stack images of whole embryo. (A,A′) E5.5, (B,B′) E6.5, (C,C′) E7.5, (D,D′) E8.0, (E-F′) E8.5, (G-G‴) E9.5 and (H-H‴) E13.5 embryos, respectively. (A-D,F,G,H) Lateral views; (E) dorsal view, (A′) bright-field view of A; (B′,C′,D′,G′,G″,H′-H″) enlarged views of the regions boxed in B,C,D,E,F,G,H, respectively. Red and green represent mCherry-hCdt1(30/120) and mVenus-hGem(1/110) signals, respectively. Scale bars: 25 μm in A; 50 μm in B; 10 μm in B′; 100 μm in C; 20 μm in C′; 100 μm in D; 200 μm in D′; 200 μm in E,F; 100 μm in E′; 50 μm in F′; 400 μm in G; 50 μm in G′,G″; 100 μm in G‴; 1 mm in H; 200 μm in H′; 400 μm in H″,H‴.

subsequent S and G_2 phases; this might be because the massive maternal mCherry-hCdt1(30/120) is carried over to the two-cell embryo (supplementary material Fig. S2G, double-arrowed lines). The signals dispersed over cytoplasm at about 18.5 hours, and the second cell division occurred 4.5 hours later; this 4.5 hours (from 18.5 hours to 23.0 hours in supplementary material Fig. S2G) is the M phase after the prophase. By contrast, the mVenus-hGem(1/110) signal was not detected at the one-cell or two-cell stage at all as in mature oocytes.

The peak intensity of mCherry-hCdt1(30/120) signal at the four-cell and eight-cell stages was comparable to that at the 16-cell stage. The mCherry-hCdt1(30/120) signal accumulated for about 2 hours at the four-cell stage and for about 3.5 hours at the eight-cell stage; these are G_1 phase (Smith and Johnson, 1986). Signals, probably due to maternal mCherry-hCdt1(30/120), were still significant in nuclei at S/G_2/M phases of the four-cell stage but residual at the eight-cell stage (supplementary material Fig. S2H,I, double-arrowed lines). mVenus-hGem(1/110) signal was observed in the nuclei of the four-cell stage embryo about 7 hours after cell division or at S phase (supplementary material Fig. S2H); it gradually increased toward M phase, though the peak intensity was yet weaker than that at the 16-cell stage, and dispersed over the cytoplasm with nuclear envelope breakdown at M phase. The signal at the eight-cell stage was almost comparable to that at the 16-cell stage. The polar body of this transgenic embryo was labeled strongly with mCherry red fluorescence but not with mVenus green.

When the *R26p-Fucci2* transgene was transmitted paternally, the signals at the 16-cell stage were almost the same as those from the transgene transmitted maternally. However, no signals were found at the one-cell or two-cell stage; the signals were weakly observed at the four-cell stage and increased during the eight-cell stage to the level at the 16-cell stage.

Fucci2 signals in *R26p-Fucci2* embryos at post-implantation stages and in adult tissues

The ubiquitous expression of Fucci2 probes in the *R26p-Fucci2* line was also examined in embryos at post-implantation stages. In E5.5 embryos, the Fucci2 fluorescence was observed in both embryonic and extra-embryonic tissues (epiblast, visceral endoderm and extra-embryonic ectoderm); the majority of the cells in each tissue exhibited mVenus-hGem(1/110) green fluorescence, and mCherry-hCdt1(30/120) red fluorescent cells were scarce (Fig. 2A, arrowheads). The E6.5 cells also exhibited mostly green fluorescence, but the red signal was apparent in the node area (Fig. 2B′, arrowheads); they were also found in some epiblast cells (Fig. 2B′, asterisk). During E7.5 to E9.5 red fluorescent cells increased in the embryonic portion, and green and red fluorescence started to establish a salt-and-pepper pattern (Fig. 2C-G). At these stages, notochord cells yielded a bright red signal; the expansion of red cells in the midline from anterior to posterior was marked (Fig. 2C′,D′, arrowheads). The cardiogenic plate also exhibited the red signal abundantly

(Fig. 2D,D′, arrows). At E8.5, bright red fluorescent cells were apparent in notochord and heart (Fig. 2E-F′), and in E9.5 embryos, the bright red signal was found in cells of rostral somites; the signal was not marked in cells of caudal somites (Fig. 2G-G″). The cells with red fluorescence were also prominent in heart (Fig. 2G,G‴), surface ectoderm in the rhombencephalic region (Fig. 2G; supplementary material Fig. S3A), otic pit (Fig. 2G; supplementary material Fig. S3B), and others. In the extra-embryonic portion the green fluorescent cells were prominent at E5.5, 6.5 and 8.0 (Fig. 2A,B,D). At E8.0 the red signal was found sporadically in the extra-embryonic portion (Fig. 2D, asterisks).

In whole-mount views of E13.5 embryos, cells with bright red fluorescence were prominent in lens primordium (Fig. 2H′; supplementary material Fig. S3D), primordium of follicles of vibrissa (Fig. 2H″), cartilage primordium of limb, and ectoderm of limb edges (Fig. 2H,H‴). The views in sections are given in supplementary material Fig. S3C-G. Bright red signals were prominent in the differentiating fields of brain and spinal cord, where cells are mostly arrested at G_1 phase (supplementary material Fig. S3C). Their proliferating ventricular zones were abundant with green signals. The green signals were also prominent in tissues such as eyes, thymus, lung, heart, stomach, intestine, tail tip and others (supplementary material Fig. S3C,E,F,G). Green signals were prominent in liver, but they were not present in nuclei and were autofluorescence; they were also seen in wild-type liver that does not harbor the *R26p-Fucci2* transgene. In adult, most of the cells exhibited bright red signals, and green signals were scarce in organs such as heart, liver, kidney and intestine (supplementary material Fig. S4A,B), suggesting that most of the cells in these organs are arrested at G_1 phase and few cells were mitotically active. However, testis exhibited green, red and yellow signals as expected (supplementary material Fig. S4B). Thus the *R26p-Fucci2* reporter must also be useful in cell cycle analysis in adult tissues.

Generation of *R26R-Fucci2* conditional reporter mouse lines

A Fucci2 mouse line was also generated by introducing the probe genes into *Rosa26* locus by homologous recombination in ES cells for the purpose of monitoring the cell cycle in a specific population of the cells in the embryo; the expressions of *mCherry-hCdt1*(*30/120*) and *mVenus-hGem*(*1/110*) were made conditional by placing the *neo* cassette (*neomycin* resistant gene directed by *PGK1* promoter with triple repeats of *SV40* polyadenylation signal) (Srinivas et al., 2001) flanked by *loxP* sequences in front of each probe (*R26R* allele; Fig. 3A). This targeting expects that the probes are expressed only when the *neo* cassette is removed by Cre-mediated *loxP* recombination (Abe et al., 2011; Srinivas et al., 2001).

Each *R26R* mouse line has been maintained in a homozygous state [*R26R-mCherry-hCdt1*(*30/120*), $Rosa26^{R\text{-}mCherry\text{-}hCdt1(30/120)/R\text{-}mCherry\text{-}hCdt1(30/120)}$; *R26R-mVenus-hGem*(*1/110*), $Rosa26^{R\text{-}mVenus\text{-}hGem(1/110)/R\text{-}mVenus\text{-}hGem(1/110)}$]. Red or green fluorescence, indicating the expression of *mCherry-hCdt1*(*30/120*) or *mVenus-hGem*(*1/110*), has never been observed in any embryos of these lines. The probe expression upon the *loxP* recombination was characterized by generating the *R26-Fucci2* mouse lines in which the *neo* cassette is deleted in all the cells of mouse by the cross with *EIIa-Cre* mice (Lakso et al., 1996); the *R26-Fucci2* mouse lines also serves as the ubiquitous cell cycle reporter line as does the *R26p-Fucci2* line. Each *R26* mouse line has been maintained in a homozygous state [*R26-mCherry-hCdt1*(*30/120*), $Rosa26^{mCherry\text{-}hCdt1(30/120)/mCherry\text{-}hCdt1(30/120)}$; *R26-mVenus-hGem*(*1/110*), $Rosa26^{mVenus\text{-}hGem(1/110)/mVenus\text{-}hGem(1/110)}$]; they are viable and fertile, exhibiting no apparent defects.

The fluorescent characteristics of each reporter line were first examined in the presence of a nuclear marker. An *R26-H2B-EGFP* male, which harbors a *H2B-EGFP* transgene at *Rosa26* locus (Abe et al., 2011), was crossed with an *R26-mCherry-hCdt1*(*30/120*) female to obtain the embryos ($Rosa26^{mCherry\text{-}hCdt1(30/120)/H2B\text{-}EGFP}$) to monitor the cell cycle behavior from the third cleavage (eight-cell stage) to blastocyst stage by time-lapse imaging (supplementary material Movie 5). mCherry-hCdt1(30/120) and H2B-EGFP signals were quantified from the third cleavage to the fifth cleavage (32-cell stage) (Fig. 3C-E). As in *R26p-Fucci2* embryos (Fig. 1E), mCherry-hCdt1(30/120) signal rapidly increased at early G_1 phase, then gradually decreased and disappeared before the cell division (Fig. 3F). The H2B-EGFP signal was detected throughout all stages of the cell cycle, and this allowed tracing of the daughter cells at each cell division. Moreover, the H2B-EGFP signal was increased transiently at metaphase, probably by chromosome condensation, so the signal intensity of H2B-EGFP fusion protein could be used as an M phase indicator. Thus *mCherry-hCdt1*(*30/120*)*/H2B-EGFP* at *Rosa26* locus monitors G_1, early S and M phases, tracing the cells over M phase to G_1 phase. The basal level of the H2B-EGFP signal increased gradually with the progress of cell cleavage, probably because of H2B-EGFP protein accumulation (Fig. 3F). During the one-cell to four-cell stage, *R26-mCherry-hCdt1*(*30/120*) embryos exhibited a strong mCherry signal when inherited maternally as *R26p-Fucci2* embryos did. The signal at the two-cell stage was more than tenfold that at the 16-cell stage (Fig. 3B); the polar body also gave a strong signal (Fig. 3B, asterisks). The signal at eight-cell stages was almost comparable to that at the 16-cell stage. Red mCherry-hCdt1(30/120) fluorescence was not detected at the one-cell or two-cell stage when inherited paternally. It was detected weakly at the four-cell stage, and increased during the eight-cell stage to the level at the 16-cell stage.

Fluorescent characteristics of *mVenus-hGem*(*1/110*) were also examined in conjunction with *H2B*-tagged *mCherry* (Fig. 3G); an *R26-H2B-mCherry* male, which harbors the *H2B-mCherry* transgene at *Rosa26* locus (Abe et al., 2011), was crossed with an *R26-mVenus-hGem*(*1/110*) female to obtain the embryos ($Rosa26^{mVenus\text{-}hGem(1/110)/H2B\text{-}mCherry}$) and to trace the cells, monitoring S, G_2 and M phases. Time-lapse imaging from fourth cleavage (16-cell stage) to blastocyst stage is given in supplementary material Movie 6, and quantification of the signals from fourth cleavage to sixth cleavage is shown in Fig. 3H-J. mVenus-hGem(1/110) signal was also observed to be similar to that in *R26p-Fucci2* embryos (Fig. 1E); after cell division the signal gradually increased and disappeared rapidly at its peak probably when nuclear envelope broke down in M phase. H2B-mCherry signal was also very similar to that of H2B-EGFP with a transient increase at metaphase. The maternal mVenus-hGem(1/110) signal was not detected at the one-cell or two-cell stage as in *R26p-Fucci2* embryos; the mVenus-hGem(1/110) signal was found weakly at the four-cell stage and at the eight-cell stage was comparable to that at the 16-cell stage. Green mVenus-hGem(1/110) fluorescence was also not detected at the one-cell or two-cell stage when inherited paternally, it was weakly found at the four-cell stage, and increased at the eight-cell stage to the level at the 16-cell stage. The green mVenus-hGem(1/110) signal was, however, detected at the two-cell stage,

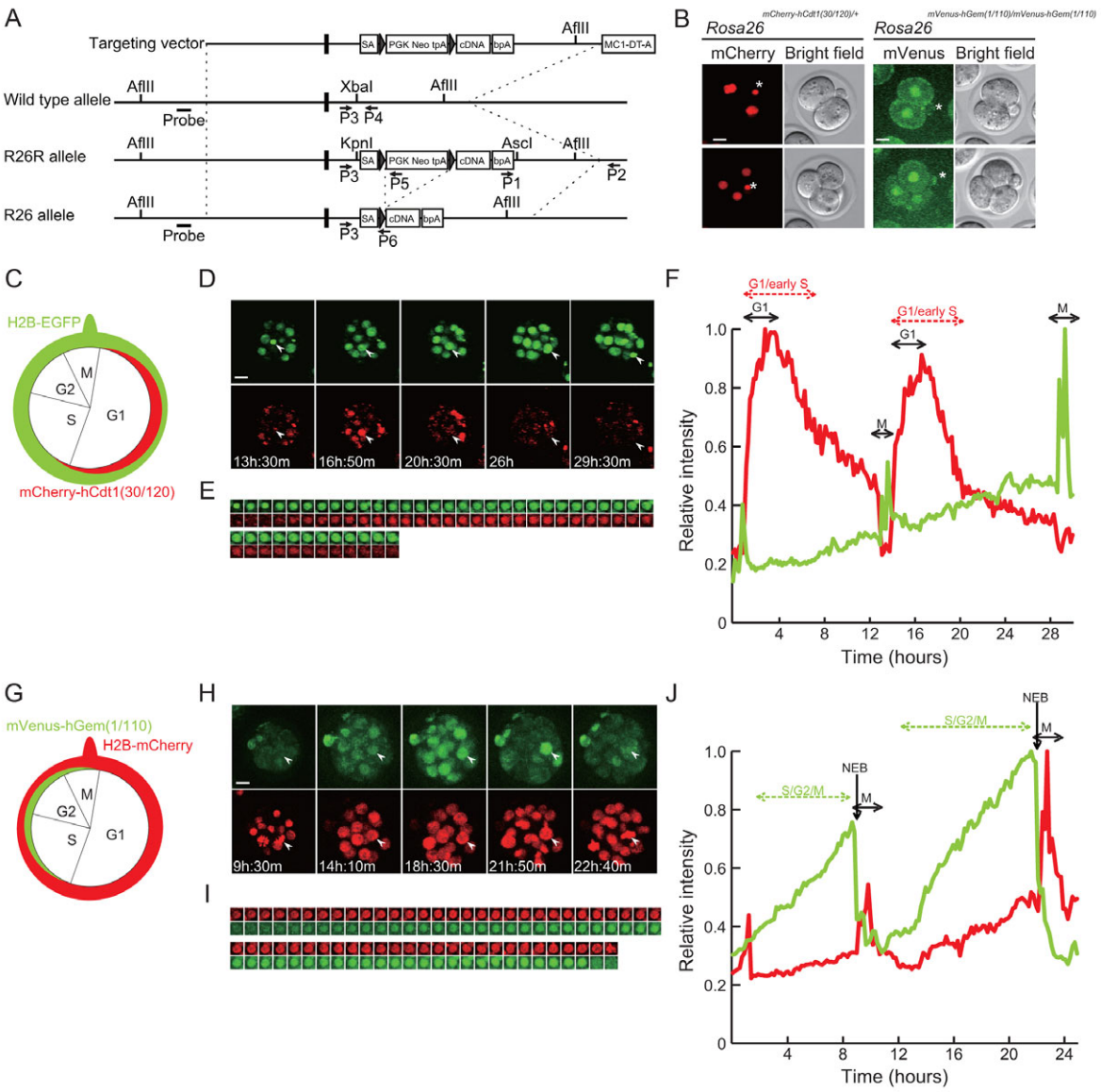

Fig. 3. Generation and characterization of *R26R-mCherry-hCdt1*(*30/120*) and *R26R-mVenus-hGem*(*1/110*) mouse lines. (**A**) Schematic of targeting vector, wild-type allele, *R26R* allele and *R26* allele. Black boxes indicate the non-coding exon 1 of the *Rosa26* locus, and black triangles *loxP* sequences. *MC1-DT-A* is a diphtheria toxin A fragment gene for negative selection directed by the *MC1* promoter (Yagi et al., 1990; Yagi et al., 1993a). cDNA represents *mCherry-hCdt1*(*30/120*) or *mVenus-hGem*(*1/110*) cDNA; *bpA*, bovine growth hormone polyadenylation sequence; *PGK Neo tpA*, neomycin resistant gene directed by *PGK1* promoter and triple repeats of *SV40* polyadenylation sequence; *SA*, adenovirus splice acceptor sequence. Probe indicates the position of the probe that is used for Southern blot analysis to identify homologous recombinants with the *Afl*II digestion. P1 and P2 are primers for PCR screening of homologous recombinant ES cells. P3, P4, P5 and P6 are PCR primers for routine genotyping of mutant mice and embryos (Abe et al., 2011). (**B**) Expression of mCherry in the heterozygous *Rosa26*$^{mCherry\text{-}hCdt1(30/120)/+}$ embryos in which *mCherry-hCdt1*(*30/120*) was transmitted maternally (left), and mVenus in the homozygous *Rosa26*$^{mVenus\text{-}hGem(1/110)/mVenus\text{-}hGem(1/110)}$ embryos (right) at the two-cell (upper panels) and four-cell (lower panels) stages. Asterisks indicate polar body. Note a high intensity of maternal mCherry expression at the two-cell stage and high backgrounds or low intensities of mVenus expression even in the homozygous state. (**C**) Diagram of mCherry-hCdt1(30/120) and H2B-EGFP expression in the *Rosa26*$^{mCherry\text{-}hCdt1(30/120)/H2B\text{-}EGFP}$ line. mCherry-hCdt1(30/120) labels G_1 and early S phase nuclei in red, whereas H2B-EGFP is expressed throughout the cell cycle with a peak at M phase. (**D**) Snapshot images of a time-lapse observation during the 16-cell stage. White arrowheads indicate nuclei that are tracked. (**E**) Higher magnification images of a nucleus indicated by arrowheads in D at 10-minute intervals. The tracked nucleus is the one indicated by white arrowheads in D. (**F**) Changes in signal intensities of mCherry-hCdt1(30/120) and H2B-EGFP probes from the third cleavage to the fifth cleavage. mCherry-hCdt1(30/120) and H2B-EGFP signals in the nucleus indicated by white arrowheads in D are given in red and green lines, respectively. (**G**) Diagram of mVenus-hGem(1/110) and H2B-mCherry expression in the *Rosa26*$^{mVenus\text{-}hGem(1/110)/H2B\text{-}mCherry}$ line. mVenus-hGem(1/110) labels S, G_2 and M phase nuclei in green, whereas H2B-mCherry is expressed throughout the cell cycle with a peak at M phase. (**H**) Snapshot images of a time-lapse observation during the 32-cell stage. White arrowheads indicate nuclei that are tracked. (**I**) Higher magnification images of a nucleus indicated by arrowheads in H at 10-minute intervals. The tracked nucleus is the one indicated by white arrowheads in H. (**J**) Changes in signal intensities of mVenus-hGem(1/110) and H2B-mCherry probes from fourth cleavage to sixth cleavage. mVenus-hGem(1/110) and H2B-mCherry signals in the nucleus indicated by white arrowheads in D are given in green and red lines, respectively. In F and J the peak intensities of mCherry, mVenus and EGFP during the observation periods are each set to 1.0, and each intensity at each time point is given as the relative value to them. Scale bars: 20 μm.

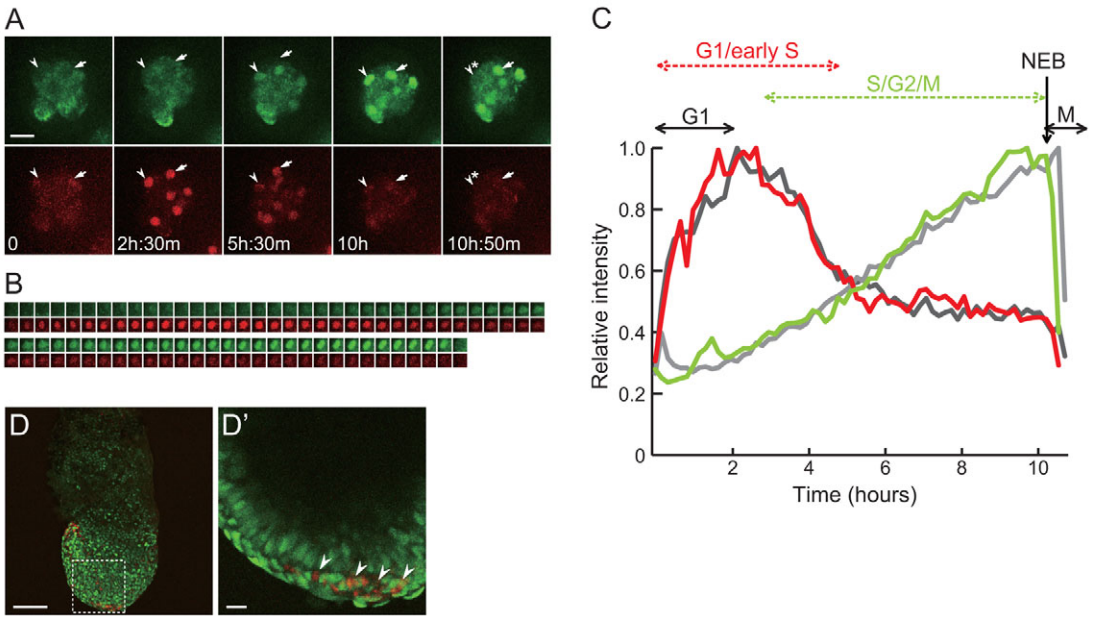

Fig. 4. Cell cycle observation by *R26-Fucci2* line. (**A**) Snapshot images of a time-lapse observation during the 16-cell stage in *R26-Fucci2* (*Rosa26*$^{mCherry\text{-}hCdt1(30/120)/mVenus\text{-}hGem(1/110)}$) embryos obtained by the cross between an *R26-mCherry-hCdt1* (*Rosa26*$^{mCherry\text{-}hCdt1(30/120)/mCherry\text{-}hCdt1(30/120)}$) female and an *R26-mVenus-hGem(1/110)* (*Rosa26*$^{mVenus\text{-}hGem(1/110)/mVenus\text{-}hGem(1/110)}$) male. White arrowheads and white arrows indicate nuclei that are tracked. (**B**) Higher magnification images of a nucleus indicated by arrowheads in A at 10-minute intervals. The tracked nucleus is the one indicated by white arrowheads in A. (**C**) Changes in signal intensities of Fucci2 probes during the 16-cell stage. mCherry-hCdt1(30/120) and mVenus-hGem(1/110) signals in the nucleus indicated by white arrowheads in A are given in red and green lines, respectively, and the nucleus indicated by white arrows in black and gray lines, respectively. The peak intensities of mCherry and mVenus at the 16-cell stage are each set to 1.0, and each intensity at each time point is given as the relative value to them. (**D**,**D′**) Fucci2 signals in an E7.5 *R26-Fucci2* embryo. D′ shows an enlarged view of the area boxed in D. Scale bars: 20 μm in A; 100 μm in D.

although weakly, in *mVenus-hGem(1/110)* homozygous (*Rosa26*$^{mVenus\text{-}hGem(1/110)/mVenus\text{-}hGem(1/110)}$) embryos (Fig. 3B); the mVenus-hGem(1/110) signal was undetectable in the polar body of the homozygotes (Fig. 3B, asterisks).

Time-lapse observation of *R26-Fucci2* embryos at preimplantation stage

The cell cycle analysis was then made with *R26-Fucci2* (*Rosa26*$^{mCherry\text{-}hCdt1(30/120)/mVenus\text{-}hGem(1/110)}$) embryos, expressing Fucci2 probes constitutively, obtained by crossing homozygous *R26-mCherry-hCdt1(30/120)* (*Rosa26*$^{mCherry\text{-}hCdt1(30/120)/mCherry\text{-}hCdt1(30/120)}$) females with homozygous *R26-mVenus-hGem(1/110)* (*Rosa26*$^{mVenus\text{-}hGem(1/110)/mVenus\text{-}hGem(1/110)}$) males or *R26-mVenus-hGem(1/110)* females with *R26-mCherry-hCdt1(30/120)* males. No difference in signals from either probe was observed at the 16-cell stage whether the probe was transmitted from maternal or paternal genome, and the following are the results in embryos obtained by the former cross.

Time-lapse imaging of the preimplantation embryos is shown in supplementary material Movie 7. The Fucci2 signals from each probe during the 16-cell stage were quantified by using captured images (Fig. 4A-C). Examples of this analysis over one cell cycle are shown in Fig. 4C. The mCherry-hCdt1(30/120) signal was detected and rapidly increased in nuclei after cell division or at G_1 phase, then slowly decreased. mVenus-hGem(1/110) signal complementarily increased, and disappeared rapidly at its peak just before cell division (Fig. 4A, asterisks). At the 16-cell stage the pattern and the intensity of mVenus-hGem(1/110) green fluorescence were comparable with that in *R26p-Fucci2* embryos (Fig. 1). The intensity of the red mCherry-hCdt1(30/120) fluorescence was, however, about half of that in *R26p-Fucci2* embryos (supplementary material Movie 7).

The pattern of Fucci2 probe expression was also examined in *R26-Fucci2* embryos at post-implantation stages; it was similar to that in *R26p-Fucci2* embryos, and an example at E7.5 is shown in Fig. 4D,D′. Most of the cells displayed green fluorescence, and red fluorescence was present in notochord (Fig. 4D′, arrowheads) cells and some epiblast cells, though less distinct than the mCherry signal in these cells of *R26p-Fucci2* embryos (Fig. 2C).

DISCUSSION

There are several advantages in the *R26p-Fucci2* line established in this study over the *CAG-Fucci* transgenic line established previously to monitor cell cycle behavior *in vivo*. The probes used, mCherry-hCdt1(30/120) and mVenus-hGem(1/110), give more distinct separation between G_1 and $S/G_2/M$ phases than mKO2-hCdt1(30/120) and mAG-hGem(1/110). *R26p-Fucci2* is more ubiquitous and intensive than *CAG-Fucci*, as represented by its expression in blastomeres at early cleavage stages and extra-embryonic tissues. The best advantage of the *R26p-Fucci2* line is that the two probes are expressed from the same transgene, whereas in *CAG-Fucci* two probe genes are inserted in different chromosomes. It is laborious to maintain the two genes together in a *CAG-Fucci* mouse line, and *R26p-Fucci2* is more useful to examine cell cycle behavior in a mutant background.

The *R26-Fucci2* (*Rosa26*$^{mCherry\text{-}hCdt1(30/120)/mVenus\text{-}hGem(1/110)}$) mice also serve as the ubiquitous cell cycle reporters; they are obtained by the cross between *R26-mCherry-hCdt1(30/120)* and *R26-*

mVenus-hGem(*1/110*) mice that are maintained homozygously. The intensity of the mVenus signal is comparable, but that of the mCherry signal is about half that in the *R26p-Fucci2* line. However, probe signals in *R26-Fucci2* may be more ubiquitous, as *Rosa26* locus is, than those in *R26p-Fucci2* generated by random transgenesis. The *R26-Fucci2* reporter will be revised in future studies by co-inserting a ubiquitous promoter such as *CAG* (Tchorz et al., 2012) and *iUBC* (Griswold et al., 2011) into the *Rosa26* locus to enhance its transcriptional activity and by making use of 2A peptide to express the two probes in a single *Rosa26* locus (Shioi et al., 2011). The greatest advantage of the knock-in *Fucci2* line is that cell cycle behavior can be examined with the parental *R26R-Fucci2* reporter in a specific population of cells by Cre-mediated cell-type-specific *loxP* recombination.

One of the difficulties in these *Fucci2* lines is the tracing of the daughter cells upon cell division, as all signals are lost. The use of a cellular marker such as H2B-EGFP and H2B-mCherry is useful to trace each daughter cell through this phase; a series of mouse lines that express each fluorescent protein in each organelle is available (Abe et al., 2011). The H2B-EGFP and H2B-mCherry signals increased transiently at metaphase probably by chromosome condensation, so their signals could be used as an M phase indicator; *mCherry-hCdt1*(*30/120*)*/H2B-EGFP* at *Rosa26* locus marks G_1, early S and M phases, tracing the cells over M phase to G_1 phase. It is also occasionally difficult to ascertain whether changes in signal intensity are due to the progression of the cell cycle or the movement of the cell or nucleus. The signal intensity of the chromosome marker is stable throughout all stages of cell cycle except for M phase, and the signal can serve to capture cells correctly.

When probe transgenes, *mCherry-hCdt1*(*30/120*) and *mVenus-hGem*(*1/110*), are transmitted paternally, their signals are not found at the one-cell or two-cell stage, are very weak at the four-cell stage and increase during the eight-cell stage to the level at the 16-cell stage. This is explained by the lack of their maternal expression, and the onset of the zygotic expression after the second cleavage (Li et al., 2010). *mVenus-hGem*(*1/110*) in both *R26p-Fucci2* and *R26-Fucci2* is also not detected at the one-cell or two-cell stage even if transmitted maternally. The mVenus-hGem(1/110) probe is not accumulated in unfertilized eggs (supplementary material Fig. S3I,I′), and the onset of the zygotic expression after the second cleavage explains this. By contrast, the G_1 phase probe mCherry-hCdt1(30/120) protein is abundantly accumulated in ooplasm when transmitted maternally (supplementary material Fig. S3H,H′), and this explains the high intensity of the mCherry-hCdt1(30/120) signal at the one-cell and two-cell stages. The maternal mCherry-hCdt1(30/120) protein and *mCherry-hCdt1*(*30/120*) mRNA might be significantly carried over to the four-cell stage, causing a considerable signal in nuclei at $S/G_2/M$ phases, and residually to the eight-cell stage. When *mCherry-hCdt1*(*30/120*) is transmitted maternally, mCherry signal is also found intensively in male pronuclei that did not have the transgene; the signal in male pronuclei must originate from maternal mCherry-hCdt1(30/120) proteins. The maternal mCherry-hCdt1(30/120) signal is also intense in the polar body.

The present study using *R26p-Fucci2* and *R26-Fucci2* reporter lines revealed the dynamic changes in cell cycle behavior during development; these reporter lines will be valuable for examining a variety of developmental processes. The G_1 phase was found to be very short, between 1.5 and 3.5 hours, in cleavage stage cells, which is consistent with the length of the G_1 phase described in previous reports (Luthardt and Donahue, 1975; Molls et al., 1983). After implantation, the red signals occurred in the node area at E6.5, and then between E7.5 to E9.5, spread over the midline structure from the anterior to posterior end. We also saw a marked increase in the number of red cells in the cardiogenic plate at this stage. Details of the cell cycle behavior during the differentiation of these tissues have been not well documented, and the analyses using the Fucci2 reporter in combination with a reporter, which is knocked-in into a gene essential for differentiation of these tissues, would be highly worthwhile. In the adult, most of the cells in each tissue exhibited red signals, consistent with a G_1-arrested state. However, in several tissues we also observed a few green cells; the Fucci2 reporters would be useful for examining the behaviors of adult stem or progenitor cells. The reporter lines will be also useful for examining the cell behavior in a variety of pathogenetic processes, such as oncogenesis in tumor-prone mice.

Acknowledgements
We acknowledge Dr Shankar Srinivas for pBigT plasmid, Dr Roger Y. Tsien for mCherry plasmid and Dr Richard R. Behringer for UBC-HS-RG plasmids.

Funding
This work was supported by an intramural grant from the Center for Developmental Biology (CDB), Riken, Kobe, Japan.

Competing interests statement
The authors declare no competing financial interests.

Supplementary material
Supplementary material available online at
http://dev.biologists.org/lookup/suppl/doi:10.1242/dev.084111/-/DC1

References
Abe, T., Kiyonari, H., Shioi, G., Inoue, K., Nakao, K., Aizawa, S. and Fujimori, T. (2011). Establishment of conditional reporter mouse lines at ROSA26 locus for live cell imaging. *Genesis* **49**, 579-590.
Friedrich, G. and Soriano, P. (1991). Promoter traps in embryonic stem cells: a genetic screen to identify and mutate developmental genes in mice. *Genes Dev.* **5**, 1513-1523.
Griswold, S. L., Sajja, K. C., Jang, C. W. and Behringer, R. R. (2011). Generation and characterization of iUBC-KikGR photoconvertible transgenic mice for live time-lapse imaging during development. *Genesis* **49**, 591-598.
Hama, H., Kurokawa, H., Kawano, H., Ando, R., Shimogori, T., Noda, H., Fukami, K., Sakaue-Sawano, A. and Miyawaki, A. (2011). Scale: a chemical approach for fluorescence imaging and reconstruction of transparent mouse brain. *Nat. Neurosci.* **14**, 1481-1488.
Karasawa, S., Araki, T., Yamamoto-Hino, M. and Miyawaki, A. (2003). A green-emitting fluorescent protein from Galaxeidae coral and its monomeric version for use in fluorescent labeling. *J. Biol. Chem.* **278**, 34167-34171.
Karasawa, S., Araki, T., Nagai, T., Mizuno, H. and Miyawaki, A. (2004). Cyan-emitting and orange-emitting fluorescent proteins as a donor/acceptor pair for fluorescence resonance energy transfer. *Biochem. J.* **381**, 307-312.
Kisseberth, W. C., Brettingen, N. T., Lohse, J. K. and Sandgren, E. P. (1999). Ubiquitous expression of marker transgenes in mice and rats. *Dev. Biol.* **214**, 128-138.
Lakso, M., Pichel, J. G., Gorman, J. R., Sauer, B., Okamoto, Y., Lee, E., Alt, F. W. and Westphal, H. (1996). Efficient *in vivo* manipulation of mouse genomic sequences at the zygote stage. *Proc. Natl. Acad. Sci. USA* **93**, 5860-5865.
Li, L., Zheng, P. and Dean, J. (2010). Maternal control of early mouse development. *Development* **137**, 859-870.
Luthardt, F. W. and Donahue, R. P. (1975). DNA synthesis in developing two-cell mouse embryos. *Dev. Biol.* **44**, 210-216.
Molls, M., Zamboglou, N. and Streffer, C. (1983). A comparison of the cell kinetics of pre-implantation mouse embryos from two different mouse strains. *Cell Tissue Kinet.* **16**, 277-283.
Nagai, T., Ibata, K., Park, E. S., Kubota, M., Mikoshiba, K. and Miyawaki, A. (2002). A variant of yellow fluorescent protein with fast and efficient maturation for cell-biological applications. *Nat. Biotechnol.* **20**, 87-90.
Niwa, H., Yamamura, K. and Miyazaki, J. (1991). Efficient selection for high-expression transfectants with a novel eukaryotic vector. *Gene* **108**, 193-199.
Potts, W., Tucker, D., Wood, H. and Martin, C. (2000). Chicken beta-globin 5′HS4 insulators function to reduce variability in transgenic founder mice. *Biochem. Biophys. Res. Commun.* **273**, 1015-1018.
Rhee, J. M., Pirity, M. K., Lackan, C. S., Long, J. Z., Kondoh, G., Takeda, J. and Hadjantonakis, A. K. (2006). *In vivo* imaging and differential localization of lipid-modified GFP-variant fusions in embryonic stem cells and mice. *Genesis* **44**, 202-218.

Sakaue-Sawano, A., Kurokawa, H., Morimura, T., Hanyu, A., Hama, H., Osawa, H., Kashiwagi, S., Fukami, K., Miyata, T., Miyoshi, H. et al. (2008). Visualizing spatiotemporal dynamics of multicellular cell-cycle progression. *Cell* **132**, 487-498.

Sakaue-Sawano, A., Kobayashi, T., Ohtawa, K. and Miyawaki, A. (2011). Drug-induced cell cycle modulation leading to cell-cycle arrest, nuclear mis-segregation, or endoreplication. *BMC Cell Biol.* **12**, 2.

Shaner, N. C., Campbell, R. E., Steinbach, P. A., Giepmans, B. N., Palmer, A. E. and Tsien, R. Y. (2004). Improved monomeric red, orange and yellow fluorescent proteins derived from Discosoma sp. red fluorescent protein. *Nat. Biotechnol.* **22**, 1567-1572.

Shioi, G., Kiyonari, H., Abe, T., Nakao, K., Fujimori, T., Jang, C. W., Huang, C. C., Akiyama, H., Behringer, R. R. and Aizawa, S. (2011). A mouse reporter line to conditionally mark nuclei and cell membranes for *in vivo* live-imaging. *Genesis* **49**, 570-578.

Smith, R. K. and Johnson, M. H. (1986). Analysis of the third and fourth cell cycles of mouse early development. *J. Reprod. Fertil.* **76**, 393-399.

Soriano, P. (1999). Generalized lacZ expression with the ROSA26 Cre reporter strain. *Nat. Genet.* **21**, 70-71.

Srinivas, S., Watanabe, T., Lin, C. S., William, C. M., Tanabe, Y., Jessell, T. M. and Costantini, F. (2001). Cre reporter strains produced by targeted insertion of EYFP and ECFP into the ROSA26 locus. *BMC Dev. Biol.* **1**, 4.

Stewart, M. D., Jang, C. W., Hong, N. W., Austin, A. P. and Behringer, R. R. (2009). Dual fluorescent protein reporters for studying cell behaviors *in vivo*. *Genesis* **47**, 708-717.

Tchorz, J. S., Suply, T., Ksiazek, I., Giachino, C., Cloëtta, D., Danzer, C. P., Doll, T., Isken, A., Lemaistre, M., Taylor, V. et al. (2012). A modified RMCE-compatible Rosa26 locus for the expression of transgenes from exogenous promoters. *PLoS ONE* **7**, e30011.

Vodermaier, H. C. (2004). APC/C and SCF: controlling each other and the cell cycle. *Curr. Biol.* **14**, R787-R796.

Yagi, T., Ikawa, Y., Yoshida, K., Shigetani, Y., Takeda, N., Mabuchi, I., Yamamoto, T. and Aizawa, S. (1990). Homologous recombination at c-fyn locus of mouse embryonic stem cells with use of diphtheria toxin A-fragment gene in negative selection. *Proc. Natl. Acad. Sci. USA* **87**, 9918-9922.

Yagi, T., Nada, S., Watanabe, N., Tamemoto, H., Kohmura, N., Ikawa, Y. and Aizawa, S. (1993a). A novel negative selection for homologous recombinants using diphtheria toxin A fragment gene. *Anal. Biochem.* **214**, 77-86.

Yagi, T., Tokunaga, T., Furuta, Y., Nada, S., Yoshida, M., Tsukada, T., Saga, Y., Takeda, N., Ikawa, Y. and Aizawa, S. (1993b). A novel ES cell line, TT2, with high germline-differentiating potency. *Anal. Biochem.* **214**, 70-76.

Zambrowicz, B. P., Imamoto, A., Fiering, S., Herzenberg, L. A., Kerr, W. G. and Soriano, P. (1997). Disruption of overlapping transcripts in the ROSA beta geo 26 gene trap strain leads to widespread expression of beta-galactosidase in mouse embryos and hematopoietic cells. *Proc. Natl. Acad. Sci. USA* **94**, 3789-3794.